Prepared in cooperation with the
NATIONAL OCEANIC AND ATMOSPHERIC ADMINISTRATION

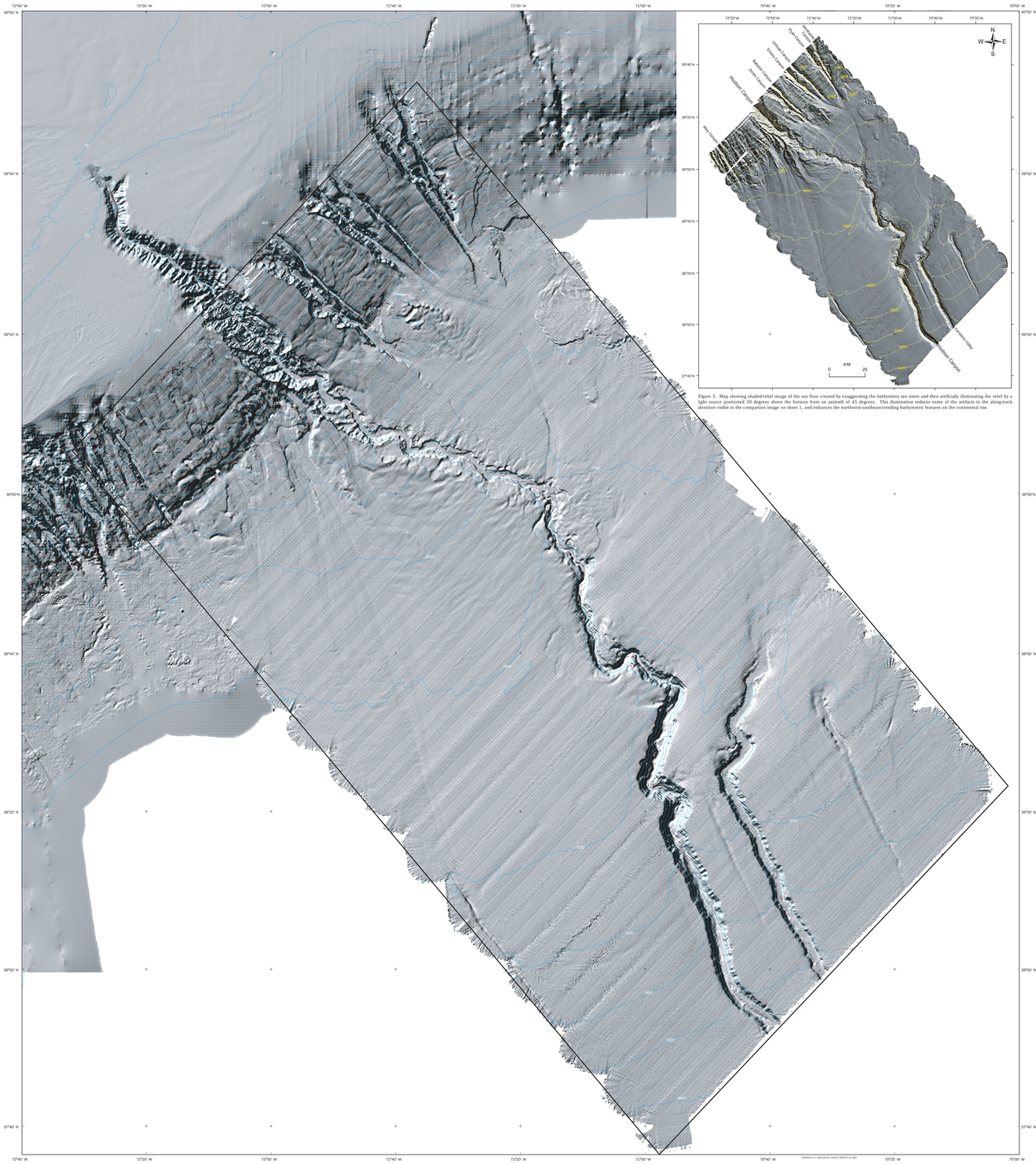

Sheet 1.—Sea floor topography in shaded relief view, with sea floor depth as topographic contours.

Any use of trade, product, or firm names in this publication is for descriptive purposes only and does not imply endorsement by the U.S. Government.

This map published on CD-ROM in pdf format.
For sale by U.S. Geological Survey, Information Services, Box 25286, Federal Center, Denver, CO 80225;
or visit http://store.usgs.gov/ or call 1-888-ASK-USGS.

For more information contact:
Bradford Butman or David C. Twichell
U.S. Geological Survey,
384 Woods Hole Road, Woods Hole, MA 02543

DISCUSSION

Introduction

These maps show the sea floor topography and backscatter intensity of the Hudson Canyon region on the continental slope and rise offshore of New Jersey and New York (Figures 1 and 2). Sheet 1 shows sea floor topography as shaded relief. Sheet 2 shows sea floor topography as shaded relief with backscatter intensity superimposed in color. Both sheets are at a scale of 1:300,000 and also show smoothed topographic contours at selected intervals. Thereupon are based on new multibeam echo-sounder data collected on an 18-day cruise carried out aboard the National Oceanic and Atmospheric Administration (NOAA) ship *Ronald H. Brown* during August and September 2002. Additional multibeam data of the Hudson Canyon collected by the Woods Hole Oceanographic Institution (WHOI), on the continental shelf collected by the STRATAFORM project (Goff and others, 1999), and a survey of the Hudson Shelf Valley (Butman and others, 2003), and a compilation of bathymetric data from the National Geophysical Data Center (NGDC) Coastal Relief Model provide coverage of areas surrounding Hudson Canyon (Figure 2). Interpretations of the surficial geology also utilize widely spaced 3.5- and 3.5-kilohertz (kHz) high-resolution seismic profiles collected by the U.S. Geological Survey (Figure 2).

Methods

A SeaBeam Instruments 2112 Multibeam Echo Sounder (12 kHz) was used to acquire the new bathymetric data on the NOAA Ship *Ronald H. Brown*. This system utilizes up to 151 electronically aimed beams spaced at intervals of 2 degrees that insonify a swath of sea floor up to 3 times the water depth. Over the continental rise, in water depths greater than about 2,000 m, a 5-km swath separation was employed, which provided almost 100% overlap of the insonified area from swath to swath. Time considerations compelled less dense coverage of the continental slope area, where a track-line separation of about 1.7 km was used that provided nearly no data overlap between swaths. The survey was conducted at approximately 10 knots (18.5 km/hr). The horizontal resolution of the beam on the sea floor ranged from about 20-65 m in the across-track direction and about 10 m in the along-track direction at 500 m water depth, and from about 100-400 m across-track and 40 m along-track at 3,000 m water depth. Vertical resolution is approximately 1% or better of the water depth. The bathymetric data are presented at a resolution of 100 m/pixel. The values are an average of the soundings within an inner 75 m circle, and a weighted average of the soundings within an outer circle that increased in size with water depth: between 500 and 1,500 m, the outer circle radius was 100 m, between 1,500 and 2,500, the radius was 200 m, and for depths greater than 2,500 m, the radius was 300 m.

Software (MB System) developed at Lamont-Doherty Earth Observatory of Columbia University was used to process and edit the bathymetric and navigation data. Software (Swath-Ed) developed by the Ocean Mapping Group at the University of New Brunswick was used to create the grids and images.

The shaded-relief image (sheet 1) was created by vertically exaggerating the topography three times and then artificially illuminating the relief by a light source positioned 45 degrees above the horizon from an azimuth of 315 degrees. To improve the dynamic range of the image, the 8-bit illumination values between 10 and 210 were stretched between 0 and 255, values below 100 were set to 0, and values above 210 were set to 255. In the resulting image, topographic features appear enhanced by strong illumination on the northwest-facing slopes and by shadows cast on southeast-facing slopes. The image also accentuates small features that could not be shown effectively by contours alone at this scale. An alternate representation of the bathymetry, without any exaggerating bathymetry ten times and then artificially illuminating the relief by a light source positioned 30 degrees above the horizon from an azimuth of 45 degrees (Figure 3), reduces the appearance of bathymetric artifacts in the along-track direction, and enhances bathymetric features that trend northwest-southeast.

Backscatter intensity (sheet 2) is a measure of surficial sediment texture and bottom roughness. Generally, high backscatter intensity is associated with rock or coarse-grained sediment and low-backscatter intensity characterizes fine-grained sediments. However, direct observations, using bottom photographs or video, or ground truth sampling techniques such as grab sampling or coring, are needed to verify such interpretations. To improve the dynamic range of the backscatter image, the 8-bit backscatter values below 180 were set to zero, values between 180 and 225 were stretched between 0 and 255, and values above 225 were set to 255. In the image shown on sheet 2, the stretched backscatter intensity is represented by a suite of eight colors ranging from blue, which represents low intensity, to red, which represents high intensity. These data are draped over the shaded-relief image. The resulting image displays light and dark tones within each color band that result from a feature's position with respect to the light source. For example, northwest-facing slopes, receiving strong illumination, show as a light tone within a color band, whereas southeast-facing slopes, being in shadow, show within a color band. An alternate backscatter-intensity image is shown on Figure 4. Here the backscatter is presented alone as a gray scale rather than being combined with the shaded-relief image as on sheet 2.

On both sheets, sea floor topography from the NGDC Coastal Relief Model (National Geophysical Data Center, 1998) is shown on the continental slope and on the continental slope to the southwest and northeast of the multibeam data (Figure 2). These data are a compilation of historical bathymetric data gridded at a resolution of 90 m/pixel. The individual points and striping in the NGDC bathymetry data appear inconsistent with adjacent multibeam values (particularly noticeable on the slope in the northeast part of sheet 1 and 2 between 70° and 72° W and north of 39° 40' N) reflect data from different sources obtained at different times with different techniques and accuracies. Data from a multibeam survey of the Hudson Shelf Valley (Butman and others, 2003) covers the head of Hudson Canyon with a resolution of 20 m/pixel and extends northeastward onto the shelf in a 20-km-wide strip. Data from a prior multibeam survey of the Hudson Canyon by researchers from the R/V Ronald H. Brown, investigators at WHOI, cover the section of Hudson Canyon from the canyon head to 3,500 m water depth in the canyon axis, but these data are shown here only between the southeastward limit of the Hudson Shelf Valley survey and the southwestern limit of the NOAA Ship *Ronald H. Brown* survey (Figure 2). Resolution of these data is 100 m/pixel. Data from a portion of a multibeam survey of the canyon floor carried out as part of the STRATAFORM project (Goff and others, 1999) occupies a triangle on the western edge of the study area, beginning near 39° 19' N, 72° 22' W. Resolution of these data is 20 m/pixel. The boundary between multibeam data and the historical NGDC data is marked by the sharp transition to increased small-scale resolution in the multibeam data.

Shaded-relief topography colored by backscatter intensity (sheet 2) is displayed only for the multibeam data collected with the SeaBeam system aboard the NOAA Ship *Ronald H. Brown* (survey area). Shaded-relief topography, based on the NGDC Coastal Relief Model and the other multibeam data, not colored by backscatter intensity, is shown by the gray tones in the area surrounding the NOAA Ship *Ronald H. Brown* survey area.

Smoothed bathymetric contours were created using ARC/INFO geographic information system software (Environmental Systems Research Institute, Inc., version 8.2). Smoothing of the multibeam bathymetric data over 500 m and the NGDC Coastal Relief Model bathymetric data over 450 m was accomplished using a rectangular 5 cell by 5 cell focal median filter. Bathymetric contours at 80 and 100 m and at 200 m intervals in depths ranging from 200 m to 3,800 m were generated from the grids using the "contour" routine in the ARC/GRID component of ARC/INFO. The contours are displayed here unedited. The contours generated from the NGDC data and the contours generated from the multibeam data do not exactly match at the boundaries of the data sets. The slope of the sea floor was computed from the smoothed bathymetric grid using Spatial Analyst in ArcGIS (Figure 5).

A streamline network was computed using the ESRI Arc Hydro Tools (version 1.1) (Figure 6). Networks that drain areas larger than 10 square km (1,000 pixels) are shown. Along-track depressions several meters deep at the outer edge of the survey tracks, caused by errors in the sound velocity, sometimes capture the streamflow in areas of flat topography, resulting in unrealistic northeast-southwest straight runs in the streamflow path. This is particularly noticeable in the southeastern portion of the survey area between 3000 and 3800 m water depth. Further editing of the multibeam data might reduce these problems. Many of the unnatural NE-SW drainage paths were visually identified and are shown in Figure 6 at reduced color intensity.

Some features in the multibeam data (sheets 1 and 2) are artifacts of data collection and environmental conditions. They include unnatural-looking features and patterns oriented parallel or perpendicular to survey track lines. On both sheets, the orientation of the track lines is identified by parallel stripes oriented northeast-southwest. Much of the striped appearance is eliminated in the shaded-relief image illuminated from the northeast, parallel to the ship track (Figure 3). In the backscatter-intensity image (sheet 2, Figure 4) track lines appear as parallel lines of noisy backscatter intensity (blue and red on sheet 2); this striping directly below the ship is particularly noticeable on the upper continental rise to the northeast and southwest of Hudson Canyon. High backscatter intensity along the floor of Hudson Canyon, particularly up-canyon, northeast, of about 39° N, appears to be interrupted by this striping. A mismatch in the time constant of the SeaBeam sonar receiver and ship autopilot, as well as some problems with the data-acquisition software, resulted in the appearance of corrugations oriented parallel to the track. These are visible principally in the shaded-relief image (sheet 1) in smooth areas of the upper rise (for example, this is particularly prominent south of 38°40' N, 71°20' W). Data collected during below 180 were set to zero, values between 180 and 225 were stretched between 0 and 255, and values above 225 were set to 255. In the image shown on sheet 2, the stretched backscatter intensity is represented by a suite of eight colors ranging from blue, which represents low intensity, to red, which represents high intensity. These data are draped over the shaded-relief image. The resulting image displays light and dark tones within each color band that result from a feature's position with respect to the light source. For example, northeast-facing slopes, receiving strong illumination, show as a light tone within a color band, whereas southeast-facing slopes, being in shadow, show within a color band. An alternate backscatter-intensity image is shown on Figure 4. Here the backscatter is presented alone as a gray scale rather than being combined with the shaded-relief image as on sheet 2.

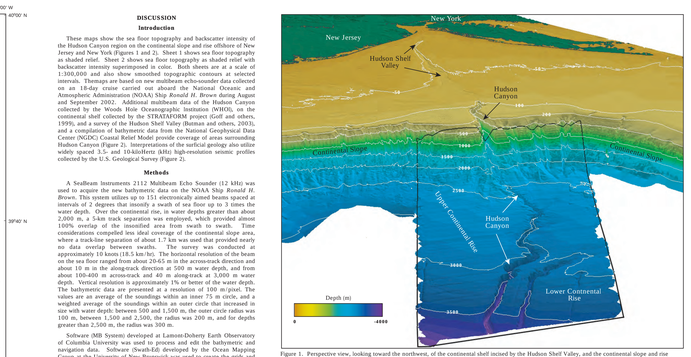

Figure 1. Perspective view, looking toward the northwest, of the continental shelf incised by the Hudson Shelf Valley, and the continental slope and rise incised by the Hudson Canyon. The black line outlines the limits of the survey carried out by the NOAA Ship *Ronald H. Brown* whose on sheets 1 and 2.

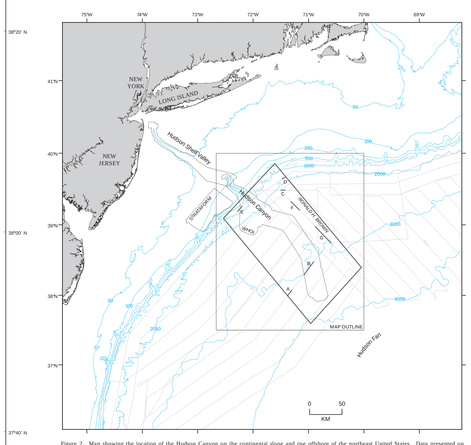

Figure 2. Map showing the location of the Hudson Canyon on the continental slope and rise offshore of the northeast United States. Data presented on sheets 1 and 2 are from the NOAA Ship *Ronald H. Brown* survey of the Hudson Canyon (outlined by the heavy black line), supplemented by multibeam surveys of the Hudson Shelf Valley (Butman and others, 2003); the Hudson Canyon (WHOI), and the outer shelf (STRATAFORM); and by the NOAA Coastal Relief Model. Light gray lines are the location of widely-spaced 3.5 kHz subbottom profiles. Lines labeled A-G are locations of profiles shown in Figure 10.

As a result of this study to commemorate geologists who pioneered studies of the US Atlantic continental margin: Kenneth O. Emery and Elazar Uchupi of Woods Hole Oceanographic Institution, William B.F. Ryan of Lamont-Doherty Earth Observatory, and Robert L. McMaster of the University of Rhode Island. The slope canyons are typically 3 to 4 km wide (rim to rim) and mostly less than 450 m deep (rim to canyon floor). McMaster Canyon merges with Ryan Canyon at about 1,900 m before reaching the base of the slope (Figures 3 and 7). All the canyons to the northeast of Hudson Canyon become narrower downslope (Figure 7). Mey Canyon, the only canyon fully in the survey area southwest of Hudson Canyon, cuts across the continental slope and extends a few kilometers onto the continental rise. Like Hudson Canyon, these canyons exhibit eroded walls and gullies indicative of slope failure. Eroded areas on the floor associated with canyons cover 13 % (3,071 km²) of the entire survey area (Table 2).

Hemipelagic Deposit

Hemipelagic sediment blankets approximately 46% of the survey area but covers only a relatively minor part of the continental slope (Figure 8). This sea floor environment has a smooth surface with a low-backscatter intensity, and on subbottom profiles it shows a series of closely spaced reflections that parallel the sea floor (Figure 10 B). Such hemipelagic sediments consist primarily of terrigenous silt and clay when sampled elsewhere on the sea floor (Dunnah, 1980). On the continental slope, hemipelagic sediment occupies the inter-canyon sections of the upper slope, and covers less of the lower part of the slope.

Scarps

An extensive but subtle network of scarps on the continental slope is revealed by the multibeam bathymetry (sheet 1, Figures 5 and 8). The shallowest of the scarps occur in 500 m water depth. Most of the scarps, which are attributed to mass wasting, are 20-75 m high (Figure 10 D, E), and the sea floor below the scarps is rough and commonly interrupted by additional scarps. The scarps outline V-shaped areas in plan view, narrowing upslope (for example, see the large scarp between Ebery and Babylon Canyons near 39° 32' N and 71° 53' W, and the scarps to the southwest of Hudson Canyon, sheet 1). The multibeam bathymetry indicates that thin-sheet slope failures have removed sediment from about 1,450 km² of the continental slope (6% of the survey area, Table 2). Multiple, sometimes intersecting scarps indicate that multi-stage collapse is commonplace on this portion of the continental slope. Seismic-reflection profiles suggest that much of the failed material was transported off the slope and deposited on the continental rise. Prior to this survey, the slope southwest of Hudson Canyon had been interpreted to be smooth based on single-beam bathymetric soundings (Uchupi and others, 2001).

Base-of-Slope Depressions

At the base of the continental slope there are a series of narrow, linear depressions (sheet 1, Figure 7). They are discontinuous, trend parallel to the base of the slope, are 0.5-2 km wide and 3-13 km long, and are as much as 23 m deeper than the surrounding sea floor. Over the section of the base of the slope that was surveyed, the depressions occur along approximately 66% of the 45-km length southwest of Hudson Canyon but only about 18% of the 65-km length to the northeast. Base-of-slope depressions have been observed southward of Mey Canyon (Robb and others, 1981; Pratson and others, 1994) and have been described as submarine plunge pools (Lee and others, 2002).

Upper Continental Rise

The upper continental rise lies seaward of the base-of-slope depressions and extends to water depths of 3,000-3,100 m. The slope of the upper rise away from submarine canyons ranges from 0.2-0.9° (Figure 5). Dendritic streamflow networks (Figure 6) drain three areas: 1) the five canyons that reach the base of the slope northward of Hudson Canyon and merge with it near 39° 03' N, 71° 16' W, 2) an area of the upper rise east of Hudson Canyon (merging with the canyon near 38° 51' N, 71° 09' W, and 3) an area of the upper rise southwest of Hudson Canyon (near 38° 39' N, 72° 08' W). A second style of drainage occupies the rise to the southwest of Hudson Canyon (in the western-most part of the map). Here, the channels are shallow, trend downslope to the south-southeast and do not coalesce in a dendritic pattern.

Hudson Canyon

Hudson Canyon extends seaward from 2,200 m water depth at the base of the continental slope, across the upper continental rise, and onto the lower rise below about 3,000-3,100m. Between the base of the continental slope near 39° 14' N, 71° 52' W and where the drainage network from the northeast merges with Hudson Canyon near 39° 01' N, 71° 16' W, the canyon trends southeast through a series of meanders with wavelengths of about 10 km. The canyon here is 2.5-11 km wide from rim to rim (Figure 9 C, D), and the average slope along this 65 km stretch is 0.6°. The canyon floor varies in width from 0.2 – 2.1 km, appears nearly flat in the shaded-relief image (sheet 1), and is floored with material showing high backscatter intensity (Figure 4, Table 1). Along this section, the north canyon rim is lower and less steep than the southern rim (Figure 9); the canyon floor is typically 50-130 m below the adjacent rise to the northeast, but 150-270 m below the rise to the south of the canyon. At the end of this section at about 2,900 m, the canyon turns nearly 90° and then runs toward the south-southeast, narrowing where it is met by the drainage from the east (near 38° 51' N, 71° 09' W). Down-canyon from this point, the canyon continues toward the south-southeast, narrows to about 5 km, and the floor is typically 400-500 m below the adjacent rise. Near 38° 37.5' N, 71° 05' W the canyon begins four sharp turns, turning first to the northeast, next to the southeast near 38° 40' N, 71° 02' W, then to the southwest near 38° 38' N, 70° 54.5' W before finally shifting back to the south-southwest near 38° 22'N, 71° W and continuing on this trend to the outer edge of the survey area. Through these turns the floor of the canyon is well defined and less than 300 m wide. The first sharp turn may be controlled by a diapiric structure that underlies this part of the valley near 38° 38' N, 71° 06' W (EEZ-Scan 87 Scientific Staff, 1991; Schlee and Robb, 1991).

Filled Valleys

Northeast of Hudson Canyon, shallow valleys which create the dendritic pattern shown on Figures 6 and 7 can be traced from the mouths of the submarine canyons at the base of the slope onto the upper rise where they coalesce into one valley; this valley then feeds into Hudson Canyon near 39° 1' N, 71° 16' W (sheet 1, Figure 7). This morphology is similar to the 'sediment-gather' areas mapped by Schlee and Robb (1991) along much of the middle Atlantic continental rise. These shallow valleys and two others on the northeastern side of Hudson Canyon (Carneros Valley and one that enters Hudson Canyon near 38° 52' N, 71° 7' W) are partially filled with mass-transport deposits (Figure 8, Figure 10 G) that were shed off the southern New England continental slope (O'Leary, 1993).

Hemipelagic Deposit

Hemipelagic sediment occurs in large patches on the upper rise on both sides of Hudson Canyon. This sedimentary facies has a smooth sea floor surface with low-backscatter intensity, and on subbottom profiles it shows a series of closely spaced reflections that parallel the sea floor (Figure 10 B). Such hemipelagic sediments consist primarily of terrigenous silt and clay in core samples from other areas (Dunnah, 1980).

Sediment Waves

A field of sediment waves lies on the upper continental rise on the southwest side of Hudson Canyon, and is shown most clearly on the image of backscatter intensity (Figure 4). The waves begin about 25 km seaward from the base of the continental slope and extend southward about 80 km across the upper rise (Figure 8). The sediment waves abut the rim of Hudson Canyon for approximately 50 km. These waves have crests oriented roughly east-west and wavelengths of 900-1,500 m. The field of sediment waves covers about 14% (3,749 km²) of the study area.

Sediment waves are known to form beneath persistent bottom currents (e.g., Rona, 1969; Mountain and Tucholke, 1983; Manson and others, 2002) and also on the levees of deep-sea channels where they are deposited from turbid flows that overtop the levees (e.g., Damuth, 1979; Normark and others, 2002). Both mechanisms probably operate in the Hudson Canyon area. Contour-following bottom currents flow to the southwest along this portion of the continental rise (e.g. Heezen and others, 1966); these currents would capture suspended sediment from the parts of down-canyon flows that rose above the canyon walls and deposit it on the rise southwest of the canyon. Similarly, the upper portions of turbidity currents that overtop the canyon walls will flow to the southwest because of the Coriolis effect. The orientation of the waves is not diagnostic of flow direction because sediment waves are known to form at nearly all angles to the prevailing currents (Flood and Hollister, 1974; Flood and Shor, 1988). Nonetheless, the slightly radiating pattern of the sediment waves (Figure 4) suggests that portions of turbid down-canyon flows escaping from the canyon near 39° N, 71° 20' W may have a dominant effect in wave formation.

Mass-Transport Deposits

Southwest of Hudson Canyon several long narrow 'fingers' of high backscatter intensity originate near the base of the slope (39° 12' N, 71° 57' W, and 39° 10' N, 72° W) and extend downslope as much as 120 km to the south in shallow depressions (sheets 1 and 2; Figures 3 and 8). Because of their distribution and backscatter pattern, these fingers are interpreted as mass-transport deposits. The surface of the ends of two of these fingers, an area covering 332 km², is covered by sediment waves (Figure 8), indicating that the surface of the mass-transport deposits was subsequently reworked by bottom currents. The average thickness of mass-transport deposits and sediment waves accounts for about 1% of the survey area. The shaded-relief and backscatter images (sheets 1 and 2, Figures 3 and 8) also show other evidence of down-slope transport from the continental slope onto the upper rise.

Northeast of Hudson Canyon there is an area of moderate to high backscatter intensity that begins at the base of the continental slope and covers most of the upper rise (Figure 4 and 8). High-resolution seismic profiles show that this area is characterized by seismically transparent layers and a rough surface (Figure 10 F, G). These layers are interpreted to be mass-transport deposits (Damuth, 1980; Figure 8). Some of the deposits were derived from the slope immediately northeast of Hudson Canyon, but a regional perspective provided by the GLORIA imagery indicates that most of the deposits were derived from the continental slope and upper rise south of New England (EEZ-Scan Scientific Staff, 1991; O'Leary, 1993). Seismic profiles show that these deposits have nearly filled the parts of the shallow valleys on the rise north of Hudson Canyon (Figure 10 G), and they extend to Hudson Canyon but do not fill it. The absence of mass-transport deposits on the floor of Hudson Canyon suggests that subsequent turbidity currents swept this material from the canyon floor. Overall, mass-transport deposits cover about 5,325 km² of the upper continental rise (20 % of the study area, Table 2).

Lower Continental Rise

The lower continental rise extends from water depths of about 3,000-3,100 m to beyond the southeastern edge of the survey area (Figure 7). The slope of the lower rise ranges from 0.5-1.2° and has, on average, but a slightly greater slope than the upper rise (Figure 5). The drainage network on the lower rise is characterized by numerous individual downslope pathways that trend toward the southeast (note that many drainage pathways in the southwest portion of the map are artifically interrupted by the along track artifacts in bathymetry shown in Figure 6).

Hudson Canyon

Hudson Canyon extends across the lower rise to beyond the southeastern limit of the survey. Over this 100 km, the canyon trends south-southeast and on aves has an average slope of 0.37 (Figure 5). The canyon is about 5 km wide from rim to rim (Figure 9). The canyon walls are 2-3 km wide and have slopes of 15-20° (Figure 5). The canyon floor is typically less than 1 km wide and 500 m below the adjacent lower rise. There is a large meander, near 38° 21.5' N, 70° 55' W that is mostly replicated by a similar meander in Carneros Valley to the northeast (sheet 1).

Hemipelagic Deposit

Hemipelagic sediment covers nearly all the lower rise except for Hudson and Carneros Canyons. This sedimentary facies has a smooth sea floor surface and low-backscatter intensity, and on subbottom profiles it shows a series of closely spaced reflections that parallel the sea floor (Figure 10 A). Such hemipelagic sediments in core samples from other areas consist primarily of terrigenous silt and clay (Damuth, 1980).

Rise Valleys

The shaded-relief maps (sheet 1, Figure 3) and the drainage network map (Figure 6) show linear valleys that originate on the lower rise in water depths between 3,000 and 3,200 m (the four largest of these valleys are shown in Figure 7). The origin of these valleys on the lower continental rise makes them distinctly different from Hudson Canyon and the other canyon-associated valleys. The rise valleys are shallow, straight features with broad, flat beds that are 6-69 m deeper than the surrounding sea floor (Figures 3 and 7). Further downslope, where they cut into the lower rise, the valleys cross than 10 m relief. High-resolution seismic profiles show that hemipelagic sedimentary layers are truncated around the heads of these valleys, indicating an erosional origin. Thinning of the layers within the valleys suggests that the valleys are maintained by preferentially reduced deposition (Figure 10 A). Farther downslope the shallowest of these valleys have subdued levees to either side, but the deeper valleys continue to have eroded walls. The rise valley at the southeastern edge of the survey area lacks a bowl-like head, and it may have been filled by mass-transport deposits (see Mass-Transport Deposits in the Upper Continental Rise section above).

The origin of the rise valleys is unknown, but the fact that they are well removed from the continental slope suggests that they are not formed by turbidity currents, which would have originated on the outer continental shelf or continental slope. Additionally, they do not appear to be the result of erosion by bottom currents, because bottom currents flow roughly perpendicular to the trend of the valleys (Heezen and others, 1966; Pratson and Laine, 1989). Pore-water discharge may be a mechanism for forming these rise valleys (Johnson, 1939; Robb, 1984). Notably, the heads of the valleys originate above the seaward edge of a major gas-hydrate proven mapped beneath the continental rise (Tucholke and others, 1977; Dillon and others, 1993). Sedimentary bedding there dips landward (Tucholke and others, 1977), so the attitude of the beds could focus fluid flow (gas and water) and stimulate sapping in this zone.

Chronology

A relative chronology can be defined from the stratigraphic stacking of the different seismic facies that are recorded on high-resolution seismic profiles. The oldest strata are those exposed by erosion along the canyon walls (Figure 10 B, C). In the section of the canyon that cuts the continental slope, these strata are of Cretaceous, Paleogene, and Neogene age (Weed and others, 1975; Gibson and others, 1968). Neogene sediments are exposed within the canyon where it crosses the continental rise (Ericson and others, 1952; Mountain and Tucholke, 1985).

The high-resolution seismic profiles have a maximum penetration of about 50 m subbottom. Although no cores from the survey area are known to be directly dated so as to provide sedimentation rates, we can infer the age of the upper 50 m of sediment from related data. Dated cores from unrended areas of the continental slope and rise to the south of our survey indicate sedimentation rates between about 5 and 15 cm/k.y. (Embley, 1980; Klasik and Pilkey, 1975). Within the survey area, mapping and interpretation of seismic stratigraphy shows that up to about 400 m of upper Pliocene and Quaternary sediments are present (Mountain and Tucholke, 1985), yielding a similar average sedimentation rate of ~11.5 cm/k.y. Thus the shallow seismic facies documented in the high-resolution profiles probably represent between 0.3 and 1.0 m.y. of sediment accumulation (*i.e.*, middle to upper Pleistocene and younger).

Scarps are cut into hemipelagic sediment on the continental slope, and they presumably reflect source areas for the mass-transport deposits that overle hemipelagic sediment in several places on the rise (Figure 10 G). These features indicate that the mass-transport deposits generally postdate the hemipelagic sediments (Figure 10 C, D). Most recently, the surfaces of some mass-transport deposits have been reworked into sediment waves, reflecting the action of overbank flow of turbidity currents and/or bottom currents, probably in the Holocene.

The shallow stratigraphy and sea-floor features show dramatic changes in the style of sedimentation during the middle to late Pleistocene and Holocene. Initially, deposits on the continental rise were a mix of turbidites and hemipelagic sediments. Turbidity currents generated on the outer shelf or upper slope were transported across the upper rise through a network of submarine canyons to the Hudson Fan seaward of the study area (Figure 2). Hudson Canyon and several canyons to the east, extending perhaps to Block Canyon, coalesced on the upper rise to form the 'gather area' that supplied sediment from a large part of the continental slope to the Hudson Fan (Schlee and Robb, 1991). Within the survey area during this time, fine-grained turbidites were deposited on the levees to either side of the canyons, and hemipelagic sediments including contourites deposited from bottom currents accumulated on the slope and on areas of the rise away from the canyons.

A period dominated by mass wasting followed the period of turbidite and hemipelagic deposition. At this time large sections of the southern New England continental slope as well as the slope to either side of Hudson Canyon failed, and the displaced sediments spread as broad sheets and fingers over large parts of the upper rise. These mass-transport deposits nearly filled all the canyons north of Hudson Canyon (Pratson and Laine, 1989; EEZ-Scan Scientific Staff, 1991; O'Leary, 1993). Turbidity currents may have been active at this time, but they were inefficient in eroding and reopening the choked portions of valleys on the rise northeast of Hudson Canyon. The age of these mass-wasting deposits is unknown, but the absence of significant sediment covering them suggests they are latest Pleistocene or early Holocene in age. It is possible that they correlate with the last lowstand of sea level, ca. 15,000 B.P., when the outermost shelf and slope were loaded with rapidly deposited, glacially and fluvially derived sediments (Emery and Uchupi, 1984; O'Leary, 1993).

A final stage of sedimentation and erosion from turbidity currents and bottom currents followed the period of mass wasting. During this period, turbidity currents appear to have been restricted largely to Hudson Canyon. Mass-transport deposits in the other canyons were relatively undisturbed, suggesting that they experienced little turbidity current activity. Along Hudson Canyon, much of the sediment in the turbid flows appears to have bypassed the upper rise and was deposited on the deeper Hudson Fan and the Hatteras Abyssal Plain. The only recognizable record of this period of sedimentation is the sediment waves southwest of Hudson Canyon, which indicates that some flows were large enough to overtop the canyon rims. The waves probably reflect reworking and deposition by a combination of the turbid flows and bottom currents. In most places, high-resolution seismic profiles do not resolve sediment covering the mass-transport deposits. However, this is not surprising if these deposits were emplaced as recently as 15,000 yr. B.P., because only about 2 m of sediment would have accumulated at the likely sedimentation rates of ~15 cm/k.y. Cores will be needed to define the timing of this and earlier stages of sedimentation more completely.

Acknowledgments

This work was supported by the NOAA Ocean Exploration program and by the U.S. Geological Survey (USGS) Coastal and Marine Geology Program. We thank the officers and crew of the NOAA Ship *Ronald H. Brown* for their assistance at sea. Peter Rona was chief scientist on the cruise. Tom Bolmer and Dave Dubois (Woods Hole Oceanographic Institution) and William Danforth (U.S. Geological Survey) assisted in data collection and processing. B. Tucholke provided multibeam from the R/V Atlantis survey for the portion of Hudson Canyon between the Hudson Shelf Valley survey and the NOAA Ship *Ronald H. Brown* survey, and Larry Mayer (University of New Hampshire) provided multibeam data from the outer shelf collected during the STRATAFORM project. B. Tucholke was supported by Office of Naval Research Grant N00014011096S and by NOAA Grant NA06RU0139, Subaward 1508 for processing and interpretation of multibeam data.

References Cited

Butman, B., Middleton, T.J., Theiler, E.R., and Schwab, W.C., 2003, Topography, Shaded Relief and Backscatter Intensity of the Hudson Shelf Valley, Offshore of New York: U.S. Geological Survey Open File Report 03-372, 1 CD-ROM. Also available on-line at http://pubs.usgs.gov/of/2003/ofr03-372/.

Damuth, J.E., 1979, Migrating sediment waves created by turbidity currents in the northern South China Basin: Geology, v. 7, p. 520-523.

Damuth, J.E., 1980, Use of high-frequency (3.5-12 kHz) echograms in the study of near-bottom sedimentation processes in the deep-sea: A review: Marine Geology, v. 38, p. 51-75.

Dillon, W.P., Fehlbaber, K., Coleman, D.F., Lee, M.W., and Hutchinson, D.R., 1995, Maps showing the gas-hydrate distribution off the east coast of the United States, U.S. Geological Survey Miscellaneous Field Studies Map MF-2268.

EEZ-Scan Scientific Staff, 1991, Atlas of the U. S. exclusive economic zone, Atlantic continental margin: U. S. Geological Survey Miscellaneous Investigation Series I-2054, 17 p.

Embley, R.W., 1980, The role of mass transport in the distribution and character of deep-ocean sediments with special reference to the North Atlantic: Marine Geology, v. 38, p. 23-50.

Emery, K.O., and Uchupi, E., 1984, The Geology of the Atlantic Ocean: New York, Springer-Verlag, 1050 p.

Ericson, D.B., Ewing, M., and Heezen, B.C., 1952, Turbidity currents and sediments in North Atlantic: American Association of Petroleum Geologists Bulletin, v. 36, p. 489-511.

Farre, J.A., McGregor, B.A., Ryan, W.B.F., and Robb, J.M., 1983, Breaching the shelfbreak: Passage from youthful to mature phase in submarine canyon evolution, *in* Stanley, D.J., and Moore, G.T., editors, The Shelfbreak: Critical Interface on Continental Margins: SEPM

Flood, R.D., and Hollister, C.D., 1974, Current-controlled topography on the continental margin off the eastern United States, *in* Burke, C.A., and Drake, C.L., editors, The Geology of Continental Margins: New York, Springer-Verlag, p. 197-205.

Flood, R.D., and Shor, A.N., 1988, Mud waves in the Argentine Basin and their relationship to regional bottom circulation patterns: Deep-Sea Research, v. 35, p. 943-971.

Gibson, T.G., Hazel, J.H., and Melo, J.F., 1968, Fossiliferous rocks from submarine canyons off the northeastern United States: U.S. Geological Survey Professional Paper 660-D, p. D222-D230.

Goff, J.A., Swift, D.J.P., Duncan, C.S., Mayer, L.A., Hughes-Clarke, J., 1999, High resolution swath sonar investigation of sand ridge, dune and ribbon morphology in the offshore environment of the New Jersey margin: Marine Geology, v. 161, p. 309-339.

Heezen, B.C., Hollister C.D., and Ruddiman, W.F., 1966, Shaping of the continental rise by deep geostrophic contour currents: Science, v. 152, p. 502-508.

Klaisk, J.A., and Pilkey, O.H., 1975, Processes of sedimentation on the Atlantic continental rise off the southeastern U.S.: Marine Geology, v. 19, p. 69-89.

Lee, S.E., Talling, P.G., Ernst, G.G.J., and Hogg, A.J., 2002, Occurrence and origin of submarine plunge pools at the base of the US continental slope: Marine Geology, v. 185, 363-377.

Mountain, G.S., and Tucholke, B.E., 1983, Abyssal sediment waves, *in* Bally, A.W., editor, Seismic Expression of Structural Styles, American Association of Petroleum Geologists Studies in Geology Series 15, p. 22-24.

Mountain, G.S. and Tucholke, B.E., 1985,Mesozoic and Cenozoic geology of the U.S. Atlantic continental slope and rise, *in*, Poag, C.W., editor, Geologic Evolution of the United States Atlantic Margin: New York, Van Nostrand Reinhold, p. 293-341.

Masson, D.G., Howe, J.A., and Stoker, M.S., 2002, Bottom-current sediment waves, sediment drifts and cemoraites in the northern Rockall Trough: Marine Geology, v. 192, p. 215-237.

National Geophysical Data Center, [1998]; NGDC Coastal Relief Model, Volumes 01 & 02, U.S. North East Atlantic Coast: [no place] National Oceanic and Atmospheric Administration, version 1.0, 1 CD-ROM. [For further information online go to http://www.ngdc.noaa.gov/mgg/coastal]

Normark, W.R., Piper, D.J.W., Posamentier, H., Pirmez, C., and Migeon, S., 2002, Variability in form and growth of sediment waves on turbidite channel levees: Marine Geology, v. 192, p. 23-58.

O'Leary, D.W., 1993, Submarine mass movement, a formative process of passive continental margins: The Munson-Nygren landslide complex and the southeast New England landslide complex, *in*, Schwab, W.C., Lee, H.J., and Twichell, D.C., editors, Submarine Landslides: Selected studies of the U.S. Exclusive Economic Zone: U. S. Geological Survey Bulletin 2002, p. 23-39.

Pratson, L.F., and Laine, E.P., 1989, The relative importance of gravity-induced versus current-controlled sedimentation during the Quaternary along the Mideast U. S. outer continental margin revealed by 3.5 kHz echo character: Marine Geology, v. 89, p. 87-126.

Pratson, L.F., Ryan, W.B.F., Mountain, G.S., and Twichell, D.C., 1994, Submarine canyon initiation by downslope-eroding sediment flows: Evidence in late Cenozoic strata on the New Jersey continental slope: Geological Society of America Bulletin, v. 106, p. 395-412.

Pratson, L.F. and Haxby, W.F., 1996, What is the slope of the U. S. continental slope?: Geology, V. 24, p. 3-6.

Robb, J.M., Kirby, J.R., and Hampson, J.C., 1981, Bathymetric map of the continental slope and uppermost continental rise between Lindenkohl Canyon and South Toms Canyon, Offshore eastern United States: U. S. Geological Survey Miscellaneous Field Studies Map MF-1270.

Rona, P.A., 1969, Linear 'lower continental rise hills' off Cape Hatteras, Journal of Sedimentary Petrology, v. 39, p. 1132-1141.

Schlee, J.S. and Robb, J.M., 1991, Submarine processes of the middle Atlantic continental rise based on GLORIA imagery: Geological Society of America Bulletin, v. 103, p. 1090-1103.

Tucholke, B.E., Bryan, G.M., and Ewing, J.I., 1977, Gas-hydrate horizons detected in seismic profiler data from the western North Atlantic: American Association of Petroleum Geologists Bulletin, v. 61, p. 698-707.